Cumhuriyet Sci. J., 43(3) (2022) 409-415
DOI: https://doi.org/10.17776/csj.1107688

Cumhuriyet Science Journal

| csj.cumhuriyet.edu.tr | Founded: 2002 ISSN: 2587-2680 e-ISSN: 2587-246X Publisher: Sivas Cumhuriyet University

Investigation of the Effect of Different Synthesis Methods on the Photocatalytic Activity of TiO_2: Comparison of Rutile and Anatase TiO_2

Fatma Kiliç Dokan [1,a,*]

[1] *Department of Chemistry and Chemical Processing Technologies, Mustafa Çıkrıkçıoglu Vocational School, Kayseri University, Kayseri, Türkiye*
**Corresponding author*

Research Article

History
Received: 22/04/2022
Accepted: 11/07/2022

ABSTRACT

In this study, the effect of the synthesis method (solid state, sol-gel and hydrothermal) on the photocatalytic activity of the anatase and rutile phases of TiO_2 was evaluated. As a result of XRD, FESEM and BET analysis of pure phase TiO_2 powders in anatase and rutile phases, the changes in particle structures, surface areas and morphologies were examined and the differences in both synthesis method and phase structures were evaluated with Photodegradation experiments. The results of the X-ray diffraction (XRD) analysis showed that the TiO_2 compound synthesized in the anatase phase and by the synthesized hydrothermal method exhibited a much smaller crystal size than the other synthesis methods and the rutile phase. Surface morphology examinations of the samples were made with scanning electron microscopy (FESEM), particle sizes were determined in the range of 90-200 nm, and their surface areas were examined by Brunauer–Emmett–Teller (BET) analysis.The adsorption-desorption isotherms shown also support the XRD data of the highest surface area.The photocatalytic behavior of the compounds was investigated using methylene blue degradation.As a result of all the syntheses and characterization studies, it has been shown that TiO_2 obtained by hydrothermal method exhibits the best photocatalytic activity.

Keywords: Anatase TiO_2, Hydrothermal method, Photocatalytic activity, Rutile TiO_2

[a] *fatmakilic@kayseri.edu.tr* *https://orcid.org/0000-0002-5355-2904*

Introduction

In different experimental research in recent years, titanium dioxide (TiO_2) has become one of the most important experimental items, mainly because of its outstanding values, including stability, non-toxic, recyclability, low cost and unique photochemical and photophysical advantages, and mainly in water-hydrogen separation, It is used as a widely applied waste treatment material. Such as water treatment, biological sensor, solar cell etc. [1-5]

Different sized inorganic materials certain structural properties structures, including nanotubes, nanorods, flower-like, fan-shaped, microspheres (hollow, solid, or porous), etc. attracted great attention due to its innovations. [6-9]

TiO_2 exists in crystalline and amorphous form. It also has three basic polymeric crystal structures: anatase, rutile, and brookite. Anatase and rutile are tetragonal, brookite is orthorhombic.

All contain the octahedral TiO6 structure, but the bond bonding is different, indicating the difference in phases; For example, the unit cell constants of rutile are a=4.59, c=2.96, while the unit cell constants of anatase are a=3.79 and c=9.51. Rutile structure is formed by the combination of 2 to 12 linear chains. The tetragonal structure is formed by the combination of oxygen atoms at the corners of these linear chains. In the anatase structure, there are no oxygen atoms at the corners and all 4 sides are tetragonal [10]. Figure 1 shows that each Ti^{4+} Ion in the crystal is surrounded by six O^{2-}. The octahedral structure in rutile crystals is not regular and shows slightly orthorhombic bending. The octahedral structure in anatase TiO_2 is greatly disturbed to a symmetry less than orthorhombic in shape, the bond length between Ti-Ti in the anatase form (3.79 Å and 3.04 Å) is greater than that of the rutile form (3.57 Å and 2.96 Å); The bond length between Ti-O (1.934 Å and 1.980 Å) is shorter than that of the rutile phase (1.949 Å and 1.980 Å) [10].

This difference in the lattice structure is the most important reason why Anatase TiO_2 is more active than rutile TiO_2 in reactions, and this causes different electronic band structure and bulk densities between the two forms of TiO_2.Rutile TiO_2 has the highest refractive index among these three phases. For this reason, it is generally used in paint raw materials and in the cosmetics industry [11] Anatase crystal form shows the highest photocatalytic activity among other crystal forms [12] For this reason, Anatase TiO_2 constitutes a large part of the studies. However, there are studies that show higher photocatalytic performance than pure Anatase, which is a mixture of Anatase and Rutile at different rates. TiO_2 nanoparticles, which are commercially used and called Degusa P-25, consist of a ratio of 3:1 (Anatase - Rutile).

Anatase TiO_2 is widely used in heterogeneous catalyst, photocatalyst, solar cells, gas sensors and wastewater treatment systems. Rutile TiO_2 has the highest refractive index among these three phases. For this reason, it is generally used in paint raw materials and in the cosmetics industry [13] Anatase crystal form shows the highest

photocatalytic activity among other crystal forms [14]. For this reason, Anatase TiO_2 constitutes a large part of the studies. However, there are studies that show higher photocatalytic performance than pure Anatase, which is a mixture of Anatase and Rutile at different rates. TiO_2 nanoparticles, which are commercially used and called Degusa P-25, consist of a ratio of 3:1 (Anatase - Rutile). Apart from the effect of different ratios in the crystal structure on the photocatalytic activity, the change in the size of the TiO_2 particles also has serious effects on the photocatalytic performance.

Particle size is a very important factor affecting the performance of photocatalytic materials. The size and type of the material directly affects the surface structure, resulting in an efficient photocatalytic material. [15-17].

In this letter, we report a solid state, sol-gel and hydrothermal approach for the synthesis of anatase and rutile TiO_2. This work will contribute to the fundamental research of different synthesis methods and the investigation and detailing of the photocatalytic activity properties on two different forms of TiO_2.

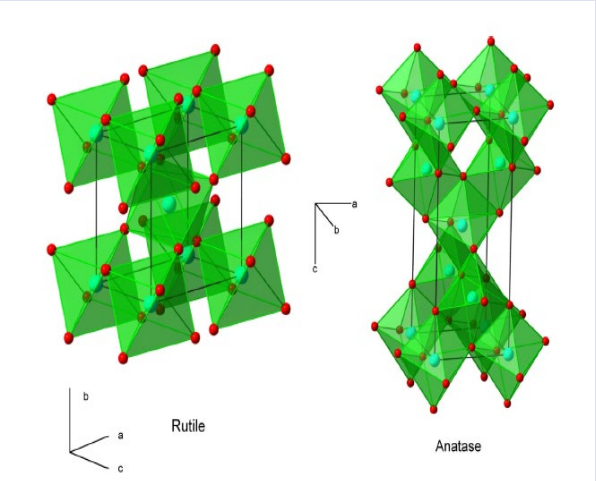

Fig.1.Rutile and anatase type of TiO_2

Materials and Methods

Synthesis of Rutile and Anatase type TiO_2

Three methods were chosen to synthesize different type of TiO_2 photocatalyst. Conventional solid state, sol-gel and new optimized hydrothermal synthesis. Dehydrate titanyl sulfate ($TiOSO_4 \cdot 2H_2O$), sodium oxalate ($Na_2C_2O_4$) and Triton -X as surfactant were used for solid state method. After grinding at room temperature for a total of 60 minutes, the precursor ($TiOC_2O_4$) was prepared. TiO_2 photocatalytic material was obtained because of heat treatment at 800°C. The material was sintered at 950°C to obtain the rutile form with the same method (fig 2.a). [18-20]

A stoichiometric amount of tetra butyl titanate was mixed vigorously into 20 mL of ethanol, and the solution was stirred continuously until gel formation. The gel was dried at 100°C, calcined at 500°C and ground to obtain TiO_2 particles (fig 2.b). [20-22]

TiO_2 synthesis was carried out with the new and optimized hydrothermal method by our team. The titanium IV butoxide and ammonia mixture was brought to the optimum pH point and mixed for 1 h at 70°C, then the stainless steel was autoclaved and heated at 180°C for 36 h. The resulting precipitate was washed 3 times to remove impurities and finally, heat treatment was carried out at 500°C for 2 hours(fig 2.c).[23]

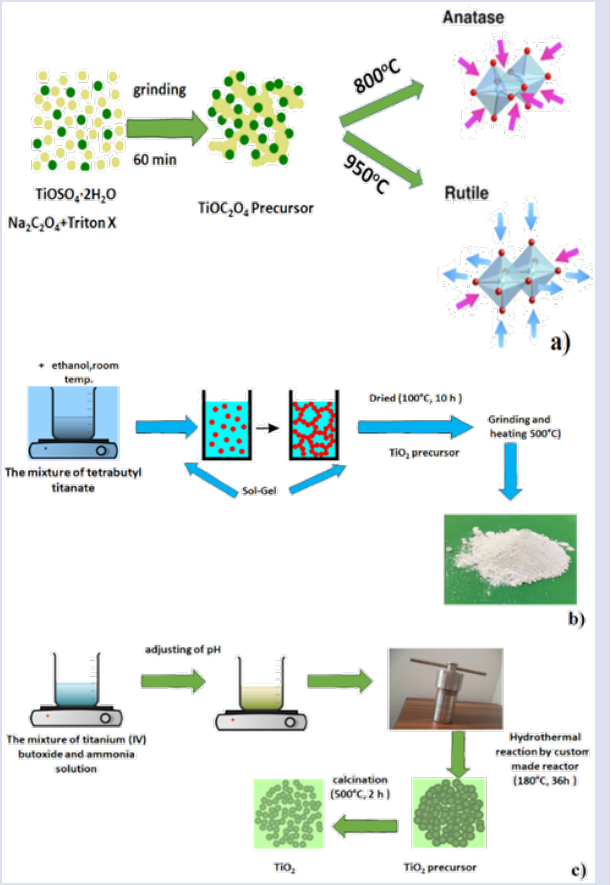

Figure 2. Schematic representation of the synthesis TiO_2 materials with different phases and method a) solid state, b) sol-gel, c) hydrothermal method

Characterization

Surface morphologies and particle distributions of TiO_2 materials synthesized by different synthesis methods (solid state, sol-gel and hydrothermal method) with different crystal phases were evaluated by Field emission scanning electron microscopy (FE-SEM, Gemini 550). The chemical components of the materials were determined by X-ray diffraction (XRD, Cu-Kα radiation, Bruker AXS D8). The bonding structures of the material were investigated in the Fourier transform infrared spectra (FT-IR) (Perkin–Elmer-spotlight 400) wavelength range of 4000–500 nm. Pore size distribution, pore volume and specific surface area were defined by the Brunauer-Emmett-Teller (BET, Gemini IV micromeritic) method.

Results

In this study, it is aimed to make comparisons by synthesizing anatase and rutil phases with all synthesis methods.

Generally, the photocatalytic activity of TiO_2 varies very significantly with the crystal phase structure, crystal size, surface area and pore structure [24]. X-ray diffraction (XRD) analysis was performed to the identification of the crystallographic structure of the samples and results can be seen in fig.3 and fig.4. In Fig 3(a-c) XRD results of the rutile phases are synthesis via different methods patterns are demonstrated. It was determined by indexing that the peaks belong to the rutile phase (JCPDS card no. 21-1276).

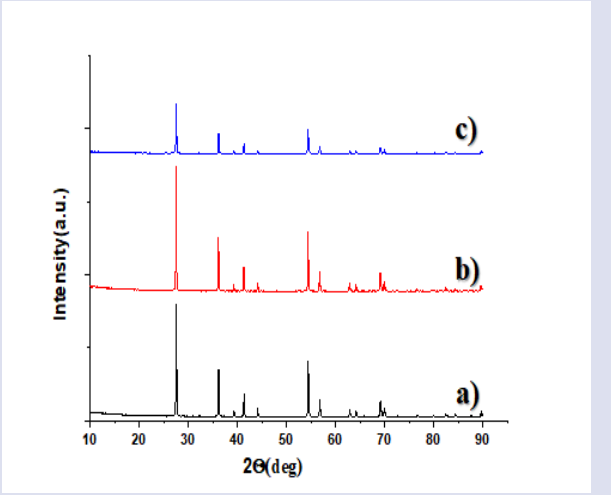

Fig.3. X-ray diffraction (XRD) pattern of the rutile TiO_2 phases synthesis via a) solid state, b) sol-gel, c) hydrothermal method

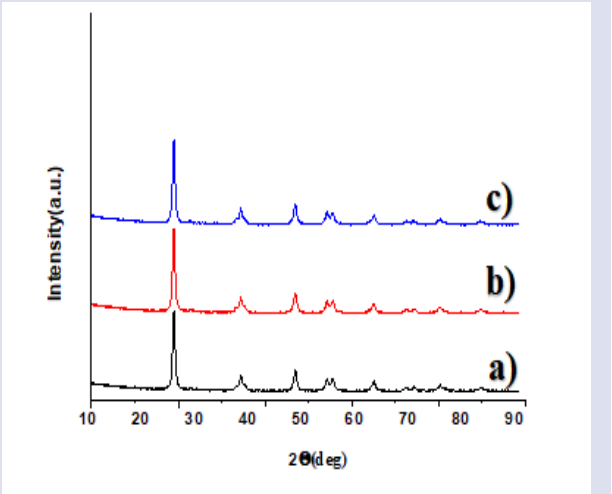

Fig.4. X-ray diffraction (XRD) pattern of anatase TiO_2 phases synthesis via a) solid state, b) sol-gel, c) hydrothermal method

The crystal structure properties of the compounds are summarized in Table 1, which shows an increase in the crystal size because of synthesis method. In Fig 4(a-c) XRD results of the anatase phases are synthesis via different methods patterns are demonstrated. All peaks that were relatively sharp compared to other peaks were first indexed as anatase TiO_2. (JCPDS No. 84-1285).

In Table 1, the crystallite sizes of all compounds synthesized by different methods are given and It is estimated from the half-bandwidth of the X-ray spectral peak by the Scherrer equation [25], which is given with Eq. 1.

$$D = \frac{0{,}94\lambda}{\beta cos\Theta} \quad (1)$$

If we examine the formula, where λ is the wavelength, Θ is the x-ray diffraction angle, β is the full width of the peaks at half maximum (FWHM) in radians. This β value was calculated from the xrd pattern with the help of the topas program. While the anatase-hydrothermal TiO_2 crystallite size is 98 nm, the rutile-solid state TiO_2 is 145 nm (Table 1). It is important that we examine table 1 to observe the effect of different synthesis methods on the crystal size.

The structure and morphology of the synthesized material were scrutinized with FESEM images(rutile) in Fig. 5 and fig 6. The FESEM image of the as-obtained TiO_2 indicates a fine spherical shape with uniform size in Fig. 5(a-c). It is observed that the spherical shape of the TiO_2 is consist of micro sphere structures.

FESEM images of the TiO_2 (anatase) exhibit that the particles had spherical morphology in low (Fig. 6 a-c) and spherical shape of the TiO_2 are consist of nano sphere structures.

Table 1. Surface area, average crystallite size, lattice parameters values for rutile and anatase TiO_2 synthesized via different methods

Sample	Surface area (m^2/g)	Average crystallite size, D (nm)	Granule size (nm)	Lattice parameters (A°) a / c
Rutile TiO_2-solid state method	11	145	200-300	4,59 / 2.95
Rutile TiO_2-sol-gel method	17	132	180-230	4.58 / 2.94
Rutile TiO_2-Hydrothermal method	28	130	150-200	4.56 / 2.93
Anatase TiO_2-solid state method	24	134	100-150	3.79 / 9.53
Anatase TiO_2- sol-gel method	32	124	80-120	3.78 / 9.52
Anatase TiO_2-Hydrothermal method	44	98	70-100	3.78 / 9.51

It is remarkable that the FESEM measurements are harmony with the synthesis methods. That is, the particle sizes of the samples synthesized by the solid-state method are the largest, and the sizes of the samples synthesized by hydrothermal are smaller than the others and these measurements were taken via image pro plus 5 program, and the values are shown in Table 1.

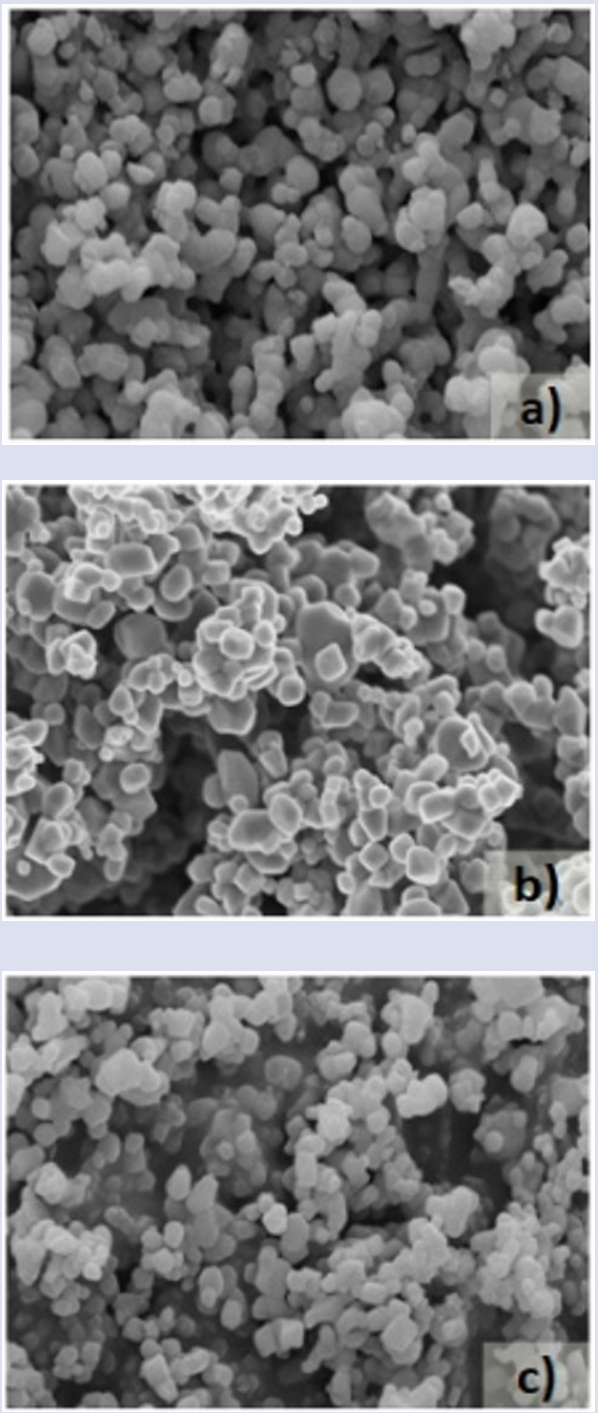

Fig. 5. FESEM images of the rutile TiO_2 phases synthesis via a) solid state, b) sol-gel, c) hydrothermal method

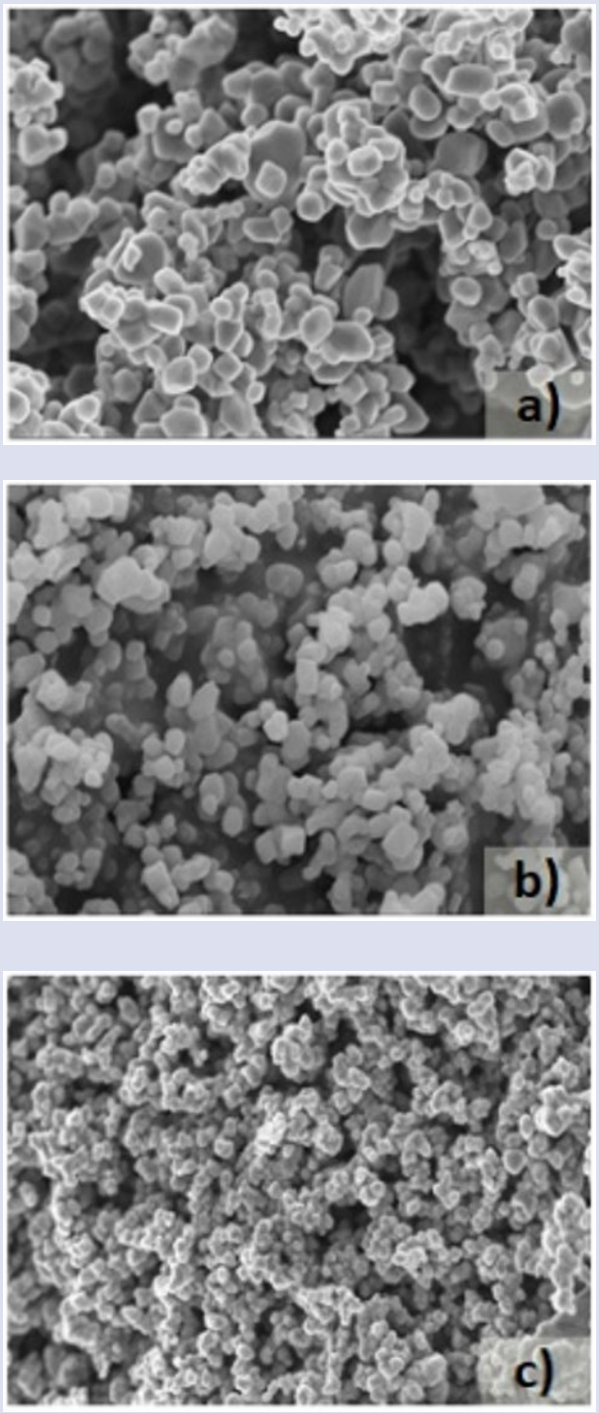

Fig. 6. FESEM images of the anatase TiO_2 phases synthesis via a) solid state, b) sol-gel, c) hydrothermal method

The crystal size values obtained from the XRD data, and the particle sizes calculated from the FESEM images are in harmony and all values are given in Table 1. To analyze the porosity of all samples N_2 adsorption-desorption isotherms were evaluated (Fig 7).

Examining the isotherm for rutile samples shows a very small, adsorbed amount of N_2 gas, indicating a non-porous property. Compared with the isotherms for anatase show a more adsorbed amount of N_2 gas indicates the existence of micropores. Average BJH adsorption pore volume values and BJH desorption pore size values are shown in Table 1.

Many different studies have suggested that TiO_2 in anatase structure generally has superior photocatalyst properties. The most important reason for this is that the anatase structure has a wider band gap, longer charge carrier lifetime, longer diffusion path length and higher charge carrier mobility. [26-33]

Therefore, the high photocataltic performance can be attributed to the outstanding structure of rutile or anatase type TiO_2.

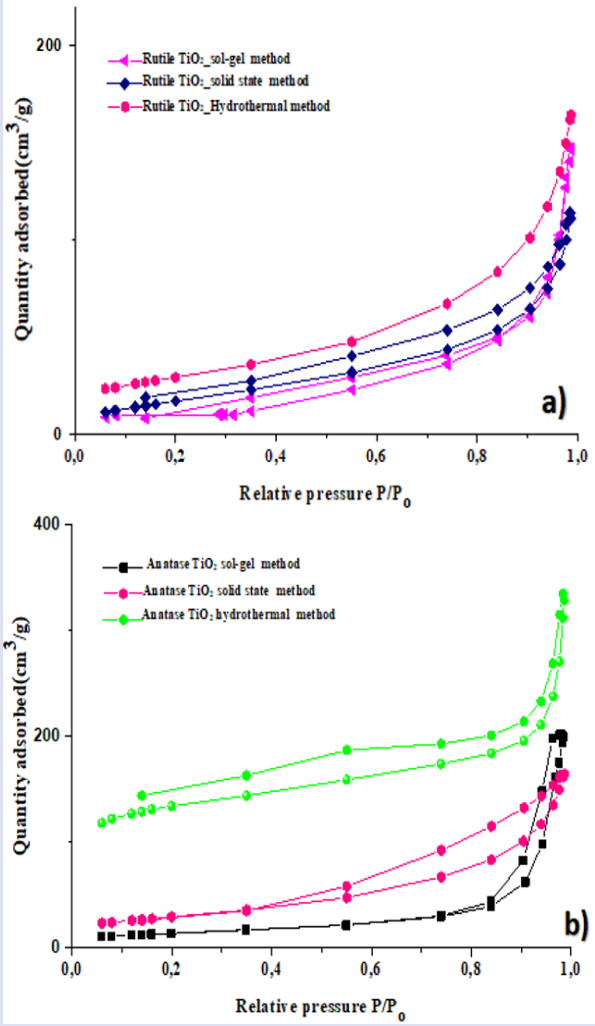

Fig. 7. Nitrogen adsorption–desorption isotherm for a)rutile and b)anatase TiO_2 synthesized via different methods.

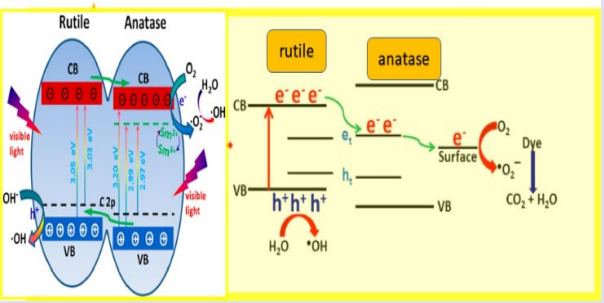

Figure 8. Schematic representation of the Difference in TiO_2 photocatalytic mechanism between rutile and anatase.

Photocatalytic activity measurements of the prepared samples were investigated by photodegradation of methylene blue (MB) using a 300 W xenon lamp. For the study, 50 mg of photocatalyst was dispersed in 100 mL of aqueous solution containing 5 ppm MB and kept in the dark for 30 min to stabilize the adsorption/desorption of the photocatalysts on the MB surface, and the photocatalytic reaction was carried out at 365 nm (15 W, under UV light).

Examining the behavior of the material without any catalyst in Figure 9.a-b, it very clearly shows that the degradation of MB is extremely slow, which means that the reduction reaction is not kinetically favorable.

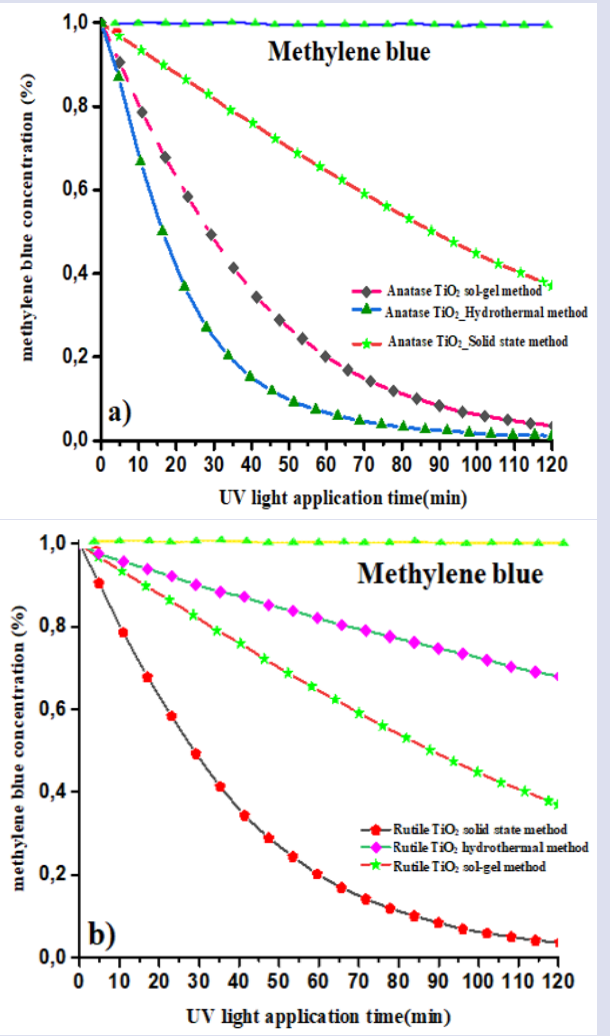

Figure.9. Degradation of methylene blue a) anatase and b) rutile TiO_2 synthesized via different methods

After adding the studied materials, a slight increase in the MB decay rate can easily be seen.

Due to the anatase structure of TiO_2, it is the most widely used semiconductor photocatalyst for the removal of organic pollutants by converting them into small molecules. Photocatalytic degradation rates of some organic pollutants are quite low. TiO_2 has a band gap of about 3.0-3.2 eV and can only be excited by light with a wavelength below 387 nm. This prevents the use of sunlight and visible light and therefore reduces the photocatalytic activity of TiO_2[34-38].

In our study, both the synthesis methods and the effects of rutile and anatase structures on the photocatalytic mechanism were investigated. Although many studies have compared rutile anatase in the literature, the synergistic effect of different synthesis methods on this mechanism has not been investigated.

When Table 1 is examined, the crystal size of the rutile phase synthesized by the hydrothermal method is small, the surface area is large and the particle size is much smaller than the other samples synthesized via sol-gel and

solid-state methods, this is an expected result because the best method used to obtain nano-sized homogeneously dispersed particles is the hydrothermal method. A different result from our expectation in the table is that the particle size of the materials obtained by the sol-gel method is larger than that obtained by the solid-state method, the possible reason for this may be the particle growth due to agglomeration during the synthesis.

Discussion and Conclusion

In this study, rutile and anatase phase TiO_2 were synthesized by different synthesis methods and the photocatalytic activities of all materials were investigated. The best result was obtained in the anatase phase synthesized by the hydrothermal method, and the lowest result was obtained in the rutile phase synthesized by the solid-state method. From the study outputs, it can be said that anatase material with a high surface area and a low crystal size is the best photocatalytic material.

Conflicts of Interest

The author declares no conflicts of interest.

Acknowledgment

The author would like to thank Nilgün Kayaci and Senem Sanduvac for their help .

References

[1] Ebrahimi M., Zakery A., Karimipour M., Molaei M., Nonlinear optical properties and optical limiting measurements of graphene oxide - Ag@TiO_2 compounds, *Opt. Mater.*, 57 (2016) 146-152.

[2] Le L., Xu J., Zhou Z., Wang H., Xiong R., Shi J., Effect of oxygen vacancies and Ag deposition on the magnetic properties of Ag/N co-doped TiO_2 single-crystal films, *Mater. Res. Bull.*, 102 (2018) 337-341.

[3] An G., Ma W., Sun Z., Liu Z., Han B., Miao S., Miao Z., Ding K., ,Preparation of titania/carbon nanotube composites using supercritical ethanol and their photocatalytic activity for phenol degradation under visible light irradiation, *Carbon* 45(9) (2007) 1795-1801.

[4] Wang T., Wei J., Shi H., Zhou M., Zhang Y., Chen Q., Zhang Z., *Physica E.*, 86 (2017) 103-110.

[5] Liu H., Dong X., Wang X., Sun C., Li J., Zhu Z., A green and direct synthesis of graphene oxide encapsulated TiO_2 core/shell structures with enhanced photoactivity, *Chem. Eng. J.*, 230 (2013) 279-285.

[6] Wang X., Li Y., Rare-Earth-Compound Nanowires, Nanotubes, and Fullerene-Like Nanoparticles: Synthesis, Characterization, and Properties., *Chem Eur J.,* 9 (22) (2003) 5627-5635.

[7] Miao-Miao Y., Zhong-Lin C., Wen-Shou W., Liang Z., Ji-Min S., Template-free Hydrothermal Preparation of Mesoporous TiO_2 Microspheres on a Large Scale., *Chemistry Letters*, 37 (9) (2008) 938-939.

[8] Wang W.S, Zhen L, Xu C.Y, Zhang B.Y, Shao W.Z., Room Temperature Synthesis of Hollow CdMoO4 Microspheres by a Surfactant-Free Aqueous Solution Route., J Phys Chem., 110 46 (2006) 23154–23158.

[9] Zhang Q., Ge J.P., Goebl J., Hu Y.X., Lu Z.D., Yin Y., Rattle-type silica colloidal particles prepared by a surface-protected etching process.,*Nano Res.*, 2 (2009) 583–591.

[10] Fujishima A., Rao T.N., Tryk D.A., TiO_2 Photocatalysts and Diamond Electrodes, *Electrochimica Acta*, 45 (28) (2000) 4683-4690.

[11] Zhao, J., Bowman L., Zhang X., Vallyathan V., Young S.H., Castranova V., ve Ding M., Titanium Dioxide (TiO_2) Nanoparticles Induce JB6 Cell Apoptosis Through Activation of the Caspase-8/Bid and Mitochondrial Pathways, *J.Toxicol. Environ. Health Part A.*,72 (19) (2009) 1141-1149.

[12] Liu X., Zhou K., Wang L., Wang B., Li Y., Oxygen Vacancy Clusters Promoting Reducibility and Activity of Ceria Nanorods, *J. Am. Chem. Soc.*, 131 (9) (2009) 3140-3141.

[13] Zhao J., Bowman L., Zhang X., Vallyathan V., Young S.H., Castranova V., Ding M.,Titanium Dioxide (TiO_2) Nanoparticles Induce JB6 Cell Apoptosis Through Activation of the Caspase-8/Bid and Mitochondrial Pathways, *J. Toxicol. Environ. Health Part A.,* 72 (19) (2009) 1141-1149.

[14] Liu L., Zhao H., Andino J.M., Li Y., Photocatalytic CO_2 Reduction with H_2O on TiO_2 Nanocrystals: Comparison of Anatase, Rutile, and Brookite Polymorphs and Exploration of Surface Chemistry, *ACS Catalysis,* 2 (8) (2012) 1817-1828.

[15] Cao S., Tao F.F., Tang Y., Li Y., Yu J., Size-and shape-dependent catalytic performances of oxidation and reduction reactions on nanocatalysts, *Chem. Soc. Rev.*, 45 (2016) 4747–4765.

[16] Hwang, Y.J., Yang, S., Lee, H., Surface analysis of N-doped TiO_2 nanorods and their enhanced photocatalytic oxidation activity, *Appl. Catal. B Environ.,* 204 (2017) 209–215.

[17] Tian, J., Zhao, Z., Kumar, A., Boughton, R.I., Liu, H., Recent progress in design, synthesis, and applications of one-dimensional TiO_2 nanostructured surface heterostructures: A review. *Chem. Soc. Rev.,* 43 (2014) 6920–6937.

[18] Zhang Z., Wang C., Zakaria R., Ying J.Y., Role of Particle Size in Nanocrystalline TiO_2-Based Photocatalysts, *J. Phys. Chem.*, 102 (1998) 10871–10878.

[19] Ohtani B., Kakimoto M., Nishimoto S., Kagiya T., Photocatalytic Reaction of Neat Alcohols by Metal-Loaded Titanium(IV) Oxide Particles, *J. Photochem. Photobiol.,* A, 70 (3) (1993) 265–72.

[20] Wang R., Hashimoto K., Fujishima A., Chikuni M., Kojima E., Kitamura A., Shimohigoshi M., Watanabe T., Photogeneration of Highly Amphiphilic TiO_2 Surfaces, *Adv. Mater.*, 10 (2) (1998) 135–38.

[21] Shklover V., Nazeeruddin M.K., Zakeeruddin S.M., Barbe C., Kay A., Haibach T., Steurer W., Hermann R., Nissen H.U., Gratzel M., Structure of Nanocrystalline TiO_2 powders and Precursor to Their Highly Efficient Photosensitizer, *Chem. Mater.*, 9 (1997) 430–39.

[22] Paratsinis S.E., Bai H., Biswas P., Kinetics of Titanium(IV) Chloride Oxidation, *J. Am. Ceram. Soc.*, 73 (7) (1990) 2158–63.

[23] Dokan F.K, Kuru M., A new approach to optimize the synthesis parameters of TiO_2 microsphere and development of photocatalytic performance, *J. Mater. Sci.: Mater. Electron,* 32 (2021) 640–65.

[24] Yu J., Yu J.C., M. Leung K.P., Ho W., Cheng B., Zhao X., Zhao J., Effects of acidic and basic hydrolysis catalysts on the photocatalytic activity and microstructures of bimodal mesoporous titania*, J. Catal.*, 217 (2003) 69.

[25] Kong M., Li Y., Chen X., Tian T., Fang P., Zheng F., Zhao X., Tuning the relative concentration ratio of bulk defects to surface defects in TiO_2 nanocrystals leads to high photocatalytic efficiency, *J. Am. Chem. Soc.*, 133 (2011) 16414–16417.

[26] Sun Q., Xu Y., Evaluating Intrinsic Photocatalytic Activities of Anatase and Rutile TiO_2 for Organic Degradation in Water, *J. Phys. Chem. C*, 114 (2010) 18911 –18918.

[27] Kavan L., Gratzel M., Gilbert S. E., Klemenz C., Scheel H.J., Electrochemical and Photoelectrochemical Investigation of Single-Crystal Anatase., *J. Am. Chem. Soc.*, 118 (1996) 6716– 6723.

[28] Batzill M., Fundamental aspects of surface engineering of transition metal oxide photocatalysts, *Energy Environ. Sci.*, 4 (2011) 3275.

[29] Fujishima A., Zhang X., Tryk D., TiO_2 photocatalysis and related surface phenomena, *Surf. Sci. Rep.*, 63 (2008) 515–582.

[30] Yamakata A., Ishibashi T., Onishi H., Time-resolved infrared absorption study of nine TiO_2 photocatalysts., *Chem. Phys.*, 339 (2007) 133 – 137.

[31] Xu M., Gao Y., Moreno E.M., Kunst M., Muhler M., Wang Y., Idriss H., Wöll C., Photocatalytic Activity of Bulk TiO_2 Anatase and Rutile Single Crystals Using Infrared Absorption Spectroscopy, *Phys. Rev. Lett.*, 106 (2011) 138302.

[32] Luttrell T., Halpegamage S., Tao J., Kramer A. Kramer, Sutter E., Batzill M., Why is anatase a better photocatalyst than rutile? - Model studies on epitaxial TiO_2 films, *Sci. Rep.*, 4 (2014) 4043.

[33] Sanjinés R., Tang H., Berger H., Gozzo F., Margaritondo G., Lévy F., Electronic structure of anatase TiO_2 oxide, *J. Appl. Phys.*, 75 (1994) 2042.

[34] Koˇcí K., Obalová L., Matˇejová L., Plachá D., Lacný Z., Jirkovský J., Šolcová O., Effect of TiO_2 particle size on the photocatalytic reduction of CO_2, *Appl. Catal. B Environ.,* 89 (2009) 494–502.

[35] Qi K., Cheng B., Yu J., Ho W., Review on the improvement of the photocatalytic and antibacterial activities of ZnO, *J. Alloys Compd.*, 727 (2017) 792–820.

[36] Mamaghani A.H., Haghighat F., Lee C.-S., Hydrothermal/solvothermal synthesis and treatment of TiO_2 for photocatalytic degradation of air pollutants: Preparation, characterization, properties, and performance, *Chemosphere*, 219 (2019) 804–825.

[37] Huang C.Y., Guo R.T., Pan W.G., Tang J.Y., Zhou W.G., Liu X.Y., Qin H., Jia P.Y., One-dimension TiO_2 nanostructures with enhanced activity for CO_2 photocatalytic reduction, *Appl. Surf. Sci.,* 464 (2019) 534–543.

[38] Liu N., Chen X., Zhang J., Schwank J.W., A review on TiO_2-based nanotubes synthesized via hydrothermal method: Formation mechanism, structure modification, and photocatalytic applications, *Catal. Today*, 225 (2014) 34–51.